Heliyon 10 (2024) e33045

Contents lists available at ScienceDirect

Heliyon

journal homepage: www.cell.com/heliyon

Research article

Comprehensive molecular analyses and experimental validation of CDCAs with potential implications in kidney renal papillary cell carcinoma prognosis

Fuping Li [a,b,1], Zhenheng Wu [c,1], Zhiyong Du [a], Qiming Ke [c], Yuxiang Fu [a], Jiali Zhan [d,*]

[a] Department of General Surgery, Shenzhen People's Hospital, The Second Clinical Medical College of Jinan University, The First Affiliated Hospital of Southern University of Science and Technology, Shenzhen, China
[b] Department of the Second Clinical Medical College, Shaanxi University of Chinese Medicine, Xianyang, China
[c] Department of Hepatobiliary Surgery, Fujian Medical University Union Hospital, Fuzhou, China
[d] Department of General Practice, Xiamen Fifth Hospital, Xiamen, China

ARTICLE INFO

Keywords:
CDCA gene family
Prognostic biomarkers
Kidney renal papillary cell carcinoma

ABSTRACT

Previous reports have revealed that the abnormal expression of the cell division cycle-associated gene family (CDCAs) is closely associated with some human cancers. However, the precise functional roles and mechanisms of CDCAs in kidney renal papillary cell carcinoma (KIRP) remain unclear. In this study, RNA sequencing data from the Cancer Genome Atlas database and Genotype-Tissue Expression databases were utilized to perform the expression, correlation, survival, mutation, functional enrichment analysis, and immunoinfiltration analyses of CDCAs in KIRP. We found that the expression levels of CDCA genes were significantly increased in KIRP across multiple databases, as confirmed by immunohistochemistry and quantitative reverse transcription PCR (RT-qPCR). Moreover, increased expression of CDCA genes is significantly associated with poor prognosis. Univariate and multivariate Cox regression analyses demonstrated that pathologic T and N staging, NUF2, CDCA2, CDCA3, CDCA5, CBX2, CDCA7, and CDCA8 were independent prognostic factors for patients with KIRP. Utilizing these nine variables, we developed a nomogram prognostic model. Furthermore, the results of GO and KEGG functional enrichment analyses suggested that CDCA genes were associated with nuclear division, mitotic nuclear division, and chromosome segregation and were involved in the cell cycle, p53 signaling pathway, and cellular senescence. We found that the expression of NUF2, CDCA2, CDCA5, and CBX2 was closely associated with the expression of lymphocytes, immunostimulatory molecules, immunoinhibitory molecules, and chemokines. In summary, NUF2, CDCA2, CDCA3, CDCA5, CBX2, CDCA7, and CDCA8 are potential biomarkers for KIRP diagnosis and prognosis.

Abbreviations: AUC, area under curve; BP, biological processes; CC, cellular components; CDCAs, cell division cycle-associated genes; CI, credible interval; FPR, false positive rate; GTEx, Genotype-Tissue Expression; GO, gene ontology; HR, hazard ratio; IHC, Immunohistochemistry; KIRP, Kidney renal papillary cell carcinoma; KEGG, kyoto encyclopedia of genes and genomes; MF, molecular function; MSI, microsatellite instability; OS, overall survival; PPI, protein-protein interaction; ROC, receiver-operating characteristic; TCGA, The Cancer Genome Atlas; TPM, transcripts per million; TMB, tumor mutational burden; TPR, true positive rate.

* Corresponding author. Xiamen Fifth Hospital, 101 Ming'an Rd, Xiamen, Fujian, 361101, China.
E-mail address: jializhan2265@163.com (J. Zhan).

[1] These authors have contributed equally to this work and are the co-first authors.

https://doi.org/10.1016/j.heliyon.2024.e33045
Received 30 March 2024; Received in revised form 29 May 2024; Accepted 13 June 2024
Available online 13 June 2024

1. Introduction

Kidney renal papillary cell carcinoma (KIRP) is a highly heterogeneous type of renal cell carcinoma and the second most frequent pathological type. It accounts for approximately 15–20 % of all kidney malignancies and exhibits low malignancy and relatively good prognosis [1]. Currently, KIRP is often detected during physical examinations due to the absence of clinical symptoms. Nephrectomy and nephron-sparing surgery are common therapeutic modalities for patients with KIRP without metastasis. Molecular targeted therapy and chemoradiotherapy have limited benefits in treating advanced metastatic KIRP [2,3]. However, the lack of accurate therapeutic targets, prognostic biomarkers, and limited preclinical models have hindered the development of effective therapies for KIRP [4]. Therefore, there is a need to identify effective and reliable biomarkers that can help improve the efficacy of KIRP treatment and the survival rate.

The cell division cycle-associated gene family (CDCAs) comprises of eight members: CDCA1 (also known NUF2), CDCA2, CDCA3, CDCA4, CDCA5, CDCA6 (also known CBX2), CDCA7, and CDCA8. Cell division is of great importance to various biological activities [5], and CDCA gene family are crucial regulators in the process of cell division and proliferation. Previous studies have demonstrated that any disorder in cell division can lead to cancer onset and progression [6,7]. Furthermore, previous reports have suggested that the aberrant expression of CDCAs is strongly correlated with some human cancers, including ovarian cancer [8], hepatocellular carcinoma [9], prostate cancer [10], nasopharyngeal carcinoma [11], breast cancer [12], pancreatic adenocarcinoma [13], stomach carcinoma [14], hypopharyngeal squamous cell carcinoma [15], and non-small cell lung cancer [16]. Notably, few studies have described the relationship between certain members of the CDCA family and the immune microenvironment. For instance, it has been reported that the upregulation of CDCA8 is closely correlated with decreased infiltration of $CD8^+$ T cells and increased infiltration of $CD4^+$ Th1 cells [11]. High CDCA7 expression may be relevant to mast cell infiltration during inflammation [14].

To date, few studies have investigated the association between the abnormal expression of CDCA gene family members and KIRP. For instance, researchers have found that the SK-RC-39 cell line is more sensitive to sunitinib after CDCA3 knockout [17]. However, the precise functional roles and mechanisms of CDCAs in KIRP remain unclear. This study aimed to explore the expression and mutations in CDCA genes and their correlation with immune infiltration in KIRP.

2. Materials and methods

2.1. Data collection and processing

The analytical process used in this study is shown in sFig. 1. The expression profiles of CDCA genes and clinical data were obtained from various databases, including The Cancer Genome Atlas (TCGA, https://cancergenome.nih.gov/) [18], Genotype-Tissue Expression (GTEx, https://gtexportal.org/) [19], and ArrayExpress (https://www.ebi.ac.uk/arrayexpress) [20]. TCGA-KIRP data comprised 289 KIRP and 32 normal specimens, and GTEx data included 28 normal samples. The cBioPortal (http://www.cbioportal.org/) database [21] was used to collect data on mutations, copy-number alterations (CNA), methylation, and clinical information on CDCAs. KIRP immunity data related to CDCA genes expression were obtained from the TISIDB database (http://cis.hku.hk/TISIDB/) [22].

2.2. Expression analysis of CDCAs in KIRP

The TCGA and GTEx databases were used to explore the mRNA levels of CDCA genes in KIRP and normal renal tissues. The "ggplot2" package of R software (version 3.6.3, http://r-project.org) was used for differential expression analysis. The Wilcoxon rank-sum test was conducted to compare the tumor and normal groups. Statistical significance was established as $P < 0.05$. Microarray data on CDCA genes were available in the ArrayExpress database. The thresholds were set as follows: $\log_2$ fold change ≥ 1 and adjusted $P < 0.05$. The receiver-operating characteristic (ROC) curve and the area under the curve (AUC) were employed to assess the diagnostic value of the CDCA genes. The AUCs were as follows: AUC (0.5–0 0.7), low accuracy; AUC (0.7–0 0.9), moderate accuracy; and AUC (0.9–1.0), high accuracy.

2.3. Correlation analysis of CDCAs and clinicopathological parameters

The GEPIA 2 database (http://gepia2.cancer-pku.cn/#index) [23] was used to determine the correlation between cancer stage and CDCA genes expression. TCGA-KIRP data were used to analyze the relationship between CDCA genes expression in KIRP tissues and their clinicopathological features, such as pathological T, N, and M staging, and gender. Boxplots drawn using the R package ggplot2 were used to visualize the above associations. The Kruskal–Wallis test was applied for multiple group comparisons. Pr (>F) < 0.05 and $P < 0.05$ indicated statistical significance.

2.4. Survival analysis and subgroup survival analysis

The survival data of patients with TCGA-KIRP were analyzed to investigate the effect of CDCA genes expression on overall survival (OS) [24]. Additionally, subgroup survival analysis was conducted based on different clinicopathological characteristics such as age (≤60 years), pathological T3 stage, and pathological stage III to identify any potential survival advantage in these subgroups.

Furthermore, we performed univariate and multivariate Cox regression analysis of the TCGA-KIRP data using the "survival" and "survminer" R packages. The median expression value of these genes was used as the cutoff threshold for the survival analysis. The results of the survival analysis were visualized using forest plots generated by the "ggplot2" R package and Kaplan–Meier (KM) curves. $P < 0.05$ was considered statistically significant.

2.5. Identification of CDCA genes and construction of a prediction model for prognosis

Based on the results of univariate Cox regression analysis, candidate genes for further investigation were selected from the CDCA gene family, that exhibited a significant correlation with survival status. Then, the LASSO-Cox regression method generated by the "glmnet" R package was used to screen the appropriate variables and construct the prediction model. The risk score was obtained for each patient using the following formula: Risk score $= \sum_{i=1}^{n} \text{coefficient}(i) \times \text{expressionvalue}(i)$, where n is the number of genes. Subsequently, the median score was used as a cutoff value to classify patients with KIRP into low- and high-risk groups. Kaplan–Meier analysis was used to compare the survival times between the two risk groups. A time-dependent ROC curve was also conducted with the aid of "survival," "survminer," and "timeROC" R packages to evaluate the discriminative ability of the prediction model.

2.6. Independent prognostic evaluation of CDCA genes and construction of nomogram

Clinical data, including pathological T and pathological N staging, of patients in TCGA-KIRP database were extracted. These variables, along with CDCA genes expression, were subjected to univariate and multivariate Cox regression analyses. To facilitate visualization and potential clinical application in predicting the prognosis of KIRP patients, a nomogram based on independent variables was constructed using the "rms" R package. The performance of the nomogram was assessed using a calibration curve analysis.

2.7. Genetic alterations and co-expression analysis

In this study, we obtained the KIRP dataset (TCGA, Firehose Legacy) comprising 280 complete samples from 293 patients using the cBioPortal database. The dataset was subjected to multiple analyses, including the generation of a gene mutation map, expression heatmap, methylation heatmap, copy number alterations, and co-expression map of the CDCA genes. A Z-score threshold of ± 1.5 was set during the above analysis. The Spearman correlation coefficient was used for co-expression analysis. The significance threshold was set at $P < 0.05$.

2.8. Protein-protein interaction (PPI) network construction and functional enrichment analysis

The PPI network between the eight proteins of the CDCA genes and their 80 frequently neighboring proteins was established using the STRING tool (https://string-db.org/) [25]. PPI pairs with a combined score >0.4 were selected for analysis. Hub genes within the PPI network were identified using the "CytoHubba" plugin of Cytoscape software (version 3.9.1, https://cytoscape.org). Additionally, the MCODE components of the PPI network were analyzed using Metascape (https://metascape.org) [26]. Subsequently, the function of the CDCAs was examined using gene ontology (GO) enrichment analysis at three levels: biology process (BP), molecular function (MF), and cellular component (CC). The Kyoto Encyclopedia of Genes and Genomes (KEGG) was used for pathway analysis. The enriched terms resulting from both GO and KEGG analyses, which were conducted using the DAVID platform (https://david.ncifcrf.gov/) [27], were visualized using the "clusterprofiler" R package.

2.9. Immune-related analysis

A 100 % stacked bar chart of immune cell-type fractions (Cibersort LM22) in the KIRP was acquired from The Cancer Immunome Atlas database (https://www.tcia.at/home) [28]. The TISIDB database was used to investigate the correlation between CDCAs expression and the immune microenvironment, including tumor-infiltrating lymphocytes (TILs), immunostimulators, immunoinhibitors, and chemokines. Additionally, correlation analysis between CDCA genes expression and tumor mutational burden (TMB), microsatellite instability (MSI), and immune checkpoints was performed using TCGA-KIRP data. The Spearman correlation coefficient was utilized for correlation analysis. Statistical significance and positive correlation were defined as $P < 0.05$ and $|R| > 0.20$, respectively. Statistical differences between two groups were compared using the Wilcoxon rank-sum test.

2.10. Immunohistochemistry (IHC)

KIRP tissue microarrays (Tissue Microarray OD-CT-UrKid03-003 and Tissue Microarray HKidC080PT01) were procured from Shanghai Outdo Biotech Company (Shanghai, China) and comprised of 20 paired KIRP tissue and adjacent non-tumorous tissue samples. The tissue microarrays were subjected to IHC using the UltraSensitive™ S–P. First, the tissue samples were dewaxed, followed by antigen retrieval and treatment with 3 % hydrogen peroxide to inactivate endogenous peroxidases. Next, the tissue samples were non-specifically blocked with skim milk for 20 min. Finally, the tissue slides were separately incubated overnight at 4 °C with antibodies targeting NUF2 (1:500, Abcam), CDCA2 (1:500, Abcam), CDCA3 (1:200, Proteintech), CDCA4 (1:200, Proteintech), CDCA5 (1;

500, Abcam), CBX2 (1:500, Abcam), CDCA7 (1:200, Affinity), and CDCA8 (1:200, Abcam). After washing, the slides were stained using a diaminobenzidine (DAB) detection kit (Gene Tech, China) and counterstained with hematoxylin. All the tissue specimens were scored independently by two experienced pathologists. The staining index was computed using the following formula: staining index = staining intensity score × proportion score of stained tumor cells. Staining intensity was graded on a scale of 0–3, with 0 indicating no staining, 1 indicating weak staining (light yellow), 2 indicating moderate staining (yellow-brown), and 3 indicating strong staining (brown). The proportion of positive tumor cells was scored on a scale of 0–4, with 0 indicating no positive tumor cells, 1 indicating <25 % positive tumor cells, 2 indicating 26%–49 % positive tumor cells, 3 indicating 50%–74 % positive tumor cells, and 4 indicating ≥75 % positive tumor cells.

2.11. Cell culture and RT-qPCR

The human renal proximal tubule epithelial (HK-2) cell line and KIRP (Caki-2) cell line were obtained from Procell Life Science&Technology Co., Ltd (Wuhan, China). The SK-RC-39 (KIRP) cell line was obtained from Shanghai Fuyu Biotechnology Co., Ltd (Shanghai, China). HK2 cells were cultured in DMEM/F12 (1:1) medium. The Caki-2 cells were cultured in McCoy's 5A medium. SK-RC-39 cells were cultured in RPMI 1640 medium. All Cell lines were cultured at 37 °C in a humidified atmosphere containing 5 % CO_2.

Total RNA was isolated from cultured cells using TRIzol reagent (Thermo Fisher Scientific, USA) and converted into cDNAs using a PrimeScript One Step RT-PCR Kit (TaKaRa, Japan), according to the manufacturer's guidelines. The cDNA template was further amplified by RT-qPCR using a SYBR Premix Dimer Eraser kit (TaKaRa, Japan). All CDCA genes expression data were normalized to GAPDH expression. Relative quantification was performed using the $2^{-\Delta\Delta Ct}$ method. Primers used for RT-qPCR are listed in sTab. 1.

2.12. Statistical analyses

All statistical analyses and visualization in this study were performed using R software (version 3.6.3) and Graphpad Prim software (version 9.0.2). Data are displayed as mean ± standard deviation (SD) for each group. An unpaired *t*-test and Wilcoxon rank-sum test

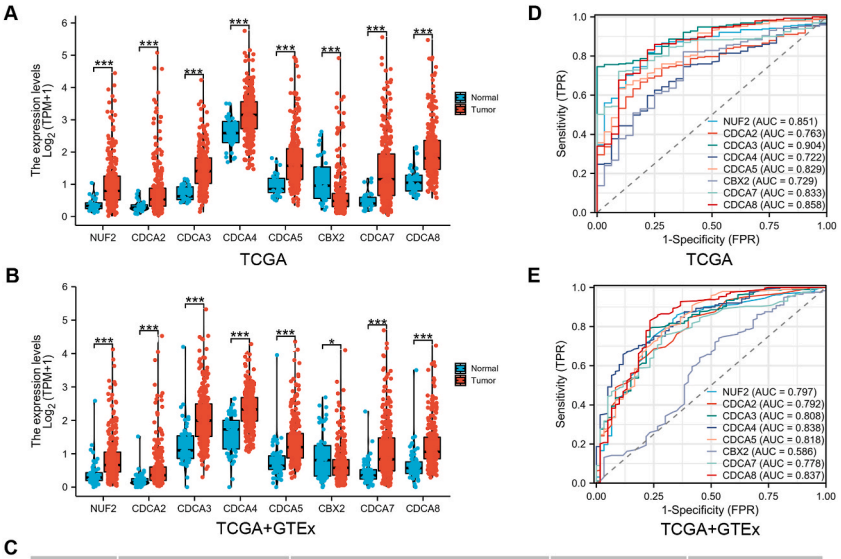

C

Gene	Experiment accession	Comparison	Log_2 fold change	Adjusted p-value
NUF2	E-GEOD-66270	Renal Carcinoma vs. Normal Tissue	1.6	1.78E-7
CDCA2	E-GEOD-66270	Renal Carcinoma vs. Normal Tissue	4.8	8.91E-15
CDCA3	E-GEOD-12606	Renal Carcinoma vs. Normal Tissue	1.1	0.041
CDCA4	E-GEOD-10927	Renal Carcinoma vs. Normal Tissue	1.5	1.11E-6
CDCA5	E-GEOD-66270	Renal Carcinoma vs. Normal Tissue	1.0	4.10E-5
CBX2	E-GEOD-48433	Renal Carcinoma vs. Normal Tissue	1.0	2.55E-4
CDCA7	E-GEOD-66270	Renal Carcinoma vs. Normal Tissue	3.3	1.41E-12
CDCA8	E-GEOD-10927	Renal Carcinoma vs. Normal Tissue	1.3	2.93E-3

ArrayExpress

Fig. 1. CDCA genes expression in KIRP and diagnostic ROC analysis. **(A)** Transcriptional levels of CDCA genes in a dataset derived from the TCGA. **(B)** Transcriptional levels of CDCA genes in a dataset derived from the TCGA + GTEx. **(C)** Transcriptional levels of CDCA genes were available in the ArrayExpress. **(D)** ROC curve for CDCA genes using the TCGA dataset. (E) ROC curve for CDCA genes using the TCGA + GTEx dataset. (*$P < 0.05$ and ***$P < 0.001$ indicated statistical significance).

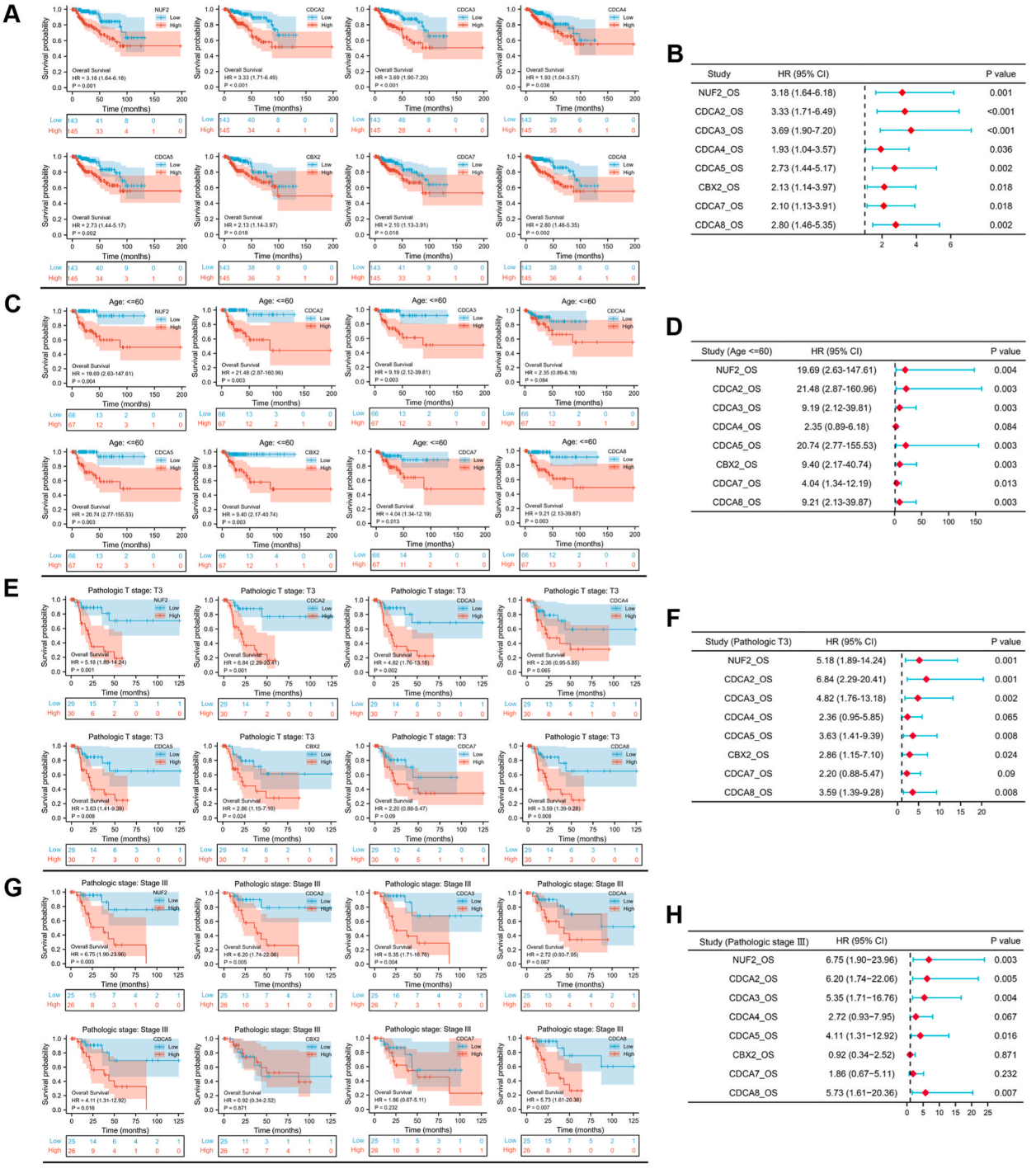

Fig. 2. The survival analysis and subgroup survival analysis for CDCA genes in patients with KIRP. **(A, B)** The Kaplan–Meier curves and forest plot for CDCA genes in KIRP. **(C, D)** The Kaplan–Meier curves and forest plot for CDCA genes in patients with KIRP younger than 60 years. **(E, F)** The Kaplan–Meier curves and forest plot for CDCA genes in patients with KIRP with pathological T3 stage. **(G, H)** The Kaplan–Meier curves and forest plot for CDCA genes in patients with KIRP with pathological stage III. ($P < 0.05$ indicated statistical significance. HR: hazard ratio. CI: credible interval).

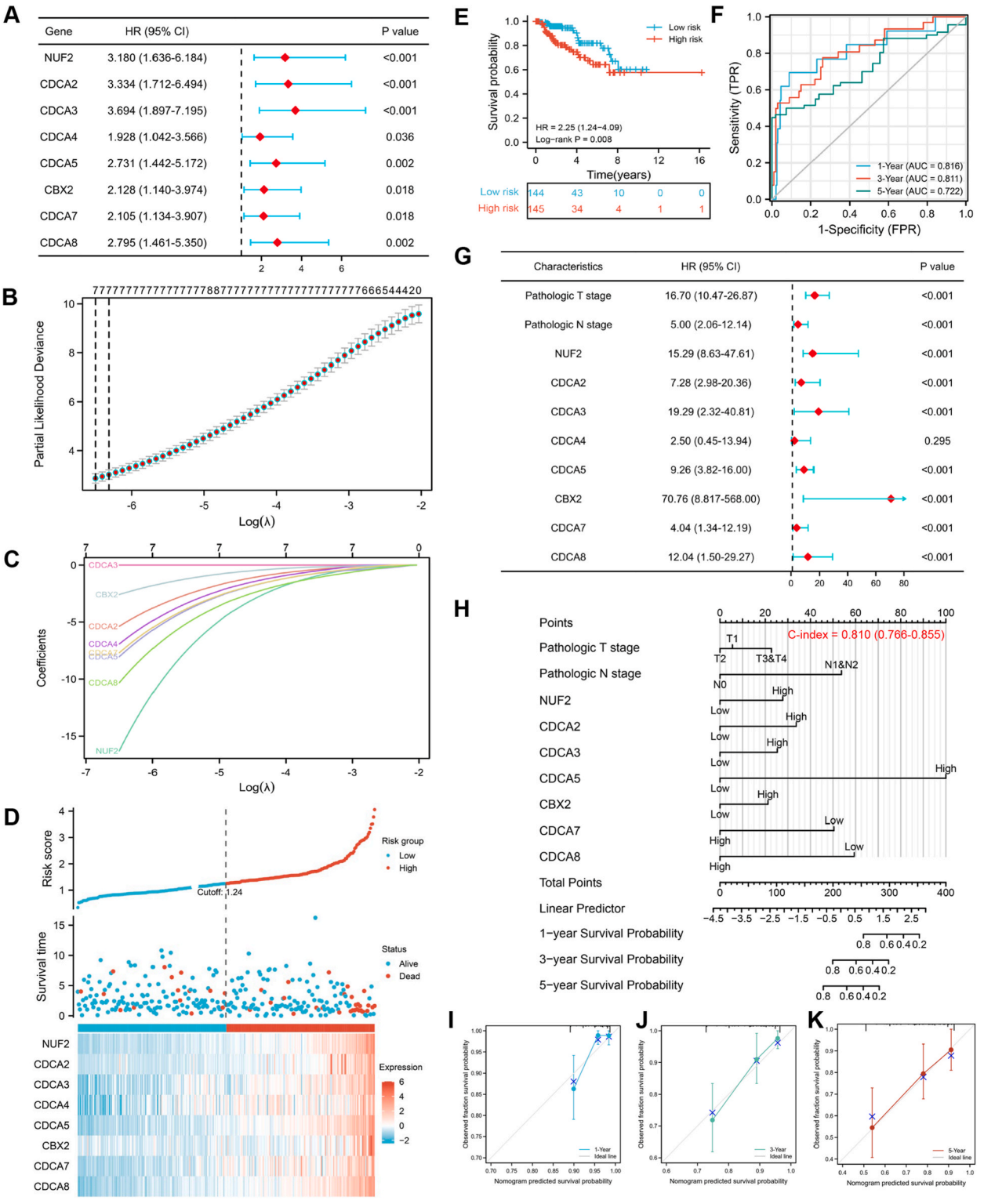

(caption on next page)

Fig. 3. Construction and assessment of the CDCAs-related risk scoring model and nomogram in patients with KIRP. **(A)** Univariate cox regression analysis of OS for CDCA genes. **(B)** LASSO coefficient profiles of the seven candidate genes. **(C)** 10-fold cross validation for tuning parameter selection in the LASSO regression. **(D)** The distribution of patient risk scores, survival status, and expression patterns of the CDCA genes for KIRP. **(E)** Kaplan-Meier survival analysis of OS for patients with KIRP in different risk groups. **(F)** Time-dependent ROC curves for 1-year, 3-year, and 5-year survival of patients with KIRP. **(G)** Multivariate cox regression analysis of OS for CDCA genes. **(H)** Nomogram for predicting 1-year, 3-year, and 5-year OS for patients with KIRP. **(I–K)** Calibration curves for 1-year, 3-year, and 5-year OS for patients with KIRP. ($P < 0.05$ indicated statistical significance. HR: hazard ratio. CI: credible interval. TPR: true positive rate. FPR: false positive rate).

tested the significance of the difference between the two groups. One-way analyses of variance (ANOVAs) and the Kruskal-Wallis test were used to test for differences in means among three or more groups. The log-rank test was used to perform the Kaplan–Meier survival analysis. Pearson correlation analysis was utilized to calculate correlation coefficients. *Z*-scores represented standard deviations from the median across samples. *A* p-value of <0.05 (two-tailed) was considered statistically significant.

3. Results

3.1. CDCA genes were overexpressed in KIRP and correlated with clinicopathological parameters

As shown in Fig. 1A and B, we first analyzed the transcriptional levels of CDCA genes using the TCGA-KIRP and TCGA normal + GTEx normal datasets. The results revealed that the expression levels of all CDCA members were significantly elevated in KIRP compared to those in normal renal tissues. Additionally, experimental data from the ArrayExpress database also further confirmed that the transcriptional levels of CDCA genes were overexpressed in KIRP (Fig. 1C). Furthermore, we assessed the diagnostic accuracy of CDCA genes for KIRP using diagnostic ROC analysis. The results of ROC analysis based on TCGA dataset showed that NUF2 (AUC = 0.851), CDCA2 (AUC = 0.763), CDCA3 (AUC = 0.904), CDCA4 (AUC = 0.722), CDCA5 (AUC = 0.829), CBX2 (AUC = 0.729), CDCA7 (AUC = 0.833), and CDCA8 (AUC = 0.858) demonstrated good diagnostic performance in distinguishing KIRP patients from healthy controls (Fig. 1D). Similarly, in the TCGA + GTEx dataset, the results of ROC analysis suggested that NUF2 (AUC = 0.797), CDCA2 (AUC = 0.792), CDCA3 (AUC = 0.808), CDCA4 (AUC = 0.838), CDCA5 (AUC = 0.818), CDCA7 (AUC = 0.778), and CDCA8 (AUC = 0.837) showed a clear distinction between KIRP patients and healthy controls (Fig. 1E).

To further evaluate the role of CDCA genes in KIRP, the correlations between CDCA genes expression and clinicopathological parameters were assessed using TCGA-KIRP dataset. As shown in sFig. 2A, the expression of CDCA genes was significantly related to cancer staging (all Pr (>F) < 0.05). Additionally, in sFig. 2B and C, the transcriptional levels of NUF2 and CDCA2/3/4/5/7/8 were significantly associated with pathological T and N staging (all $P < 0.05$). Similarly, as shown in sFig. 2D, NUF2 and CDCA2/3/4/5/8 mRNA levels were significantly relevant to pathological M staging (all $P < 0.05$). The expression levels of CDCA2/5/7/8 in female KIRP patients were meaningfully higher than those in male KIRP patients (all $P < 0.05$, sFig. 2E).

3.2. Prognostic potential of CDCAs in KIRP patients

Kaplan–Meier analyses were used to assess the prognostic value of CDCA genes expression in KIRP. As illustrated in Fig. 2A and B, high expression of CDCA genes was significantly correlated with worse OS (all $P < 0.05$). Meanwhile, subgroup survival analysis was conducted based on different clinicopathological features such as age (≤60 years), pathological T3 stage, and pathological stage III to identify any potential survival advantage in these subgroups. For age, higher expressions of NUF2, CBX2, and CDCA2/3/5/7/8 were meaningfully relevant to poorer OS in KIRP patients younger than 60 years (all $P < 0.05$; Fig. 2C and D). For pathological T staging, higher expressions of NUF2, CBX2, and CDCA2/3/5/8 were strongly associated with lower OS in KIRP patients with pathological T3 stage (all $P < 0.05$; Fig. 2E and F). For pathological stages, higher expressions of NUF2 and CDCA2/3/5/8 were significantly correlated with worse OS in KIRP patients with pathological stage III (all $P < 0.05$; Fig. 2G and H).

3.3. Construction and assessment of the CDCAs-related risk scoring model

Clinical data and prognostic information of 289 patients with KIRP (sTab. 2) were acquired from TCGA for the Cox regression analysis. Based on univariate Cox regression analysis (sTab. 3), eight potential risk genes related to OS were screened out using the cut-off values of Cox $P < 0.05$ and $HR > 1$ (Fig. 3A). Subsequently, LASSO Cox regression analysis was performed to identify survival-associated predictive genes. Seven key genes were screened for developing a CDCAs-related risk scoring model based on the minimal criteria of λ (Fig. 3B and C). To calculate the risk score for each sample, the following formula was utilized: Risk score = ([-1-16.2907130 × NUF2 expression value] + [−5.372395 × CDCA2 expression value] + [−6.922951 × CDCA4 expression value] + [−8.037803 × CDCA5 expression value] + [−2.585058 × CBX2 expression value] + [−7.693133 × CDCA7 expression value] + [−10.322759 × CDCA8 expression value]). Subsequently, a median risk score of 1.24 was used to divide KIRP patients into high- and low-risk groups (144 in the low-risk group and 145 in the high-risk group) (Fig. 3D). Patients in the high-risk group had considerably worse survival outcomes ($HR = 2.25$, Log-rank $P = 0.008$, Fig. 3E). Next, time-dependent ROC analysis was performed. The AUCs for 1-, 3-, and 5-year survival rates were 0.816, 0.811, and 0.722, respectively (Fig. 3F). Overall, the above findings suggested that the CDCAs-related risk scoring model had good predictive accuracy for the OS of patients with KIRP.

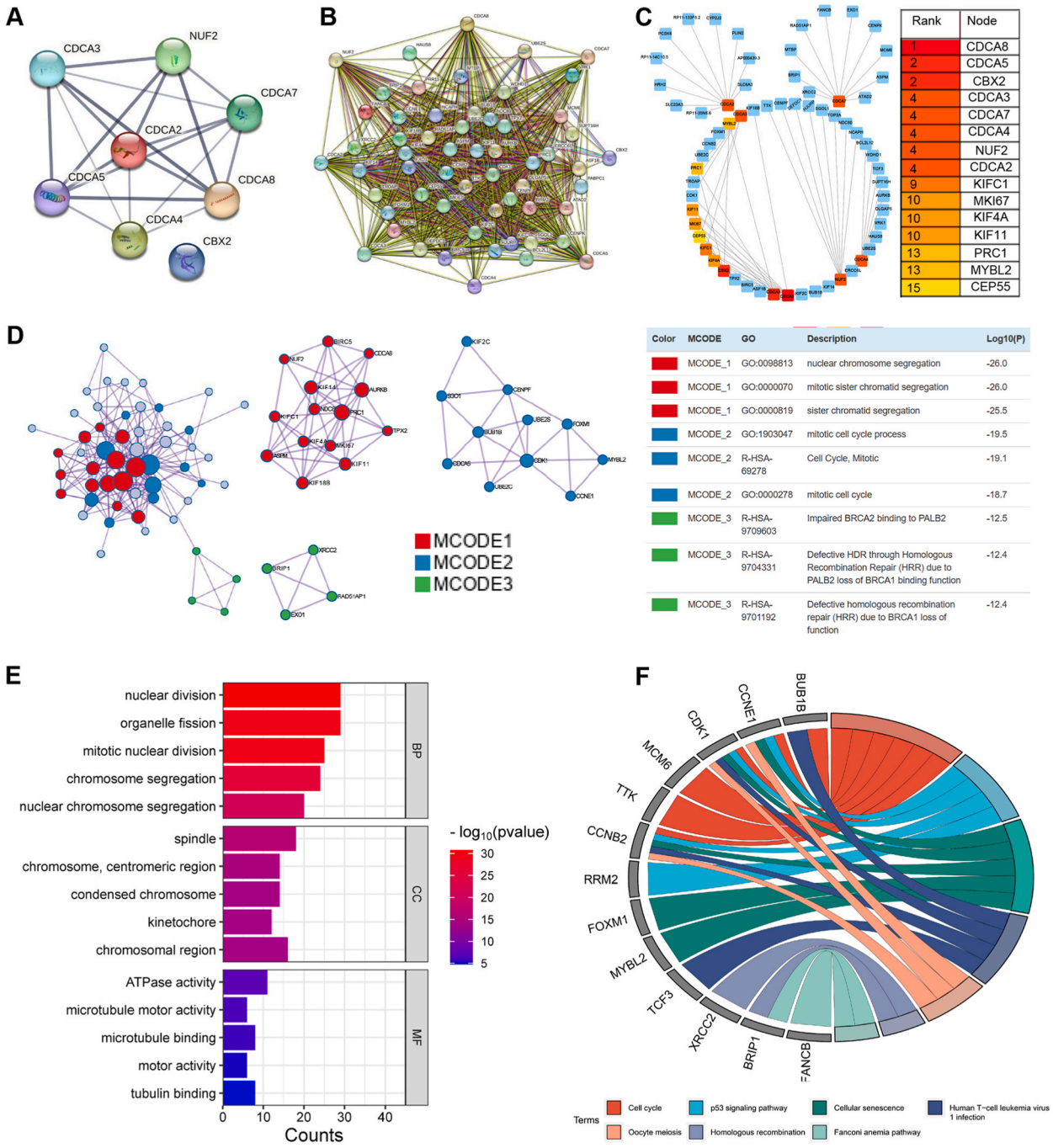

Fig. 4. Gene biological functions and interactions of CDCA genes in patients with KIRP. **(A)** PPI network based on the eight CDCA proteins. **(B)** PPI network for CDCA proteins and the 80 most frequently neighboring proteins. **(C)** The hub genes identified with Cytoscape for CDCA genes and the 80 most frequently neighboring genes. **(D)** Three most significant MCODE components form PPI network and function enrichment analysis of three MCODE components independently among CDCA genes and the 80 most frequently neighboring genes. **(E, F)** GO and KEGG functional enrichment analyses of CDCAs.

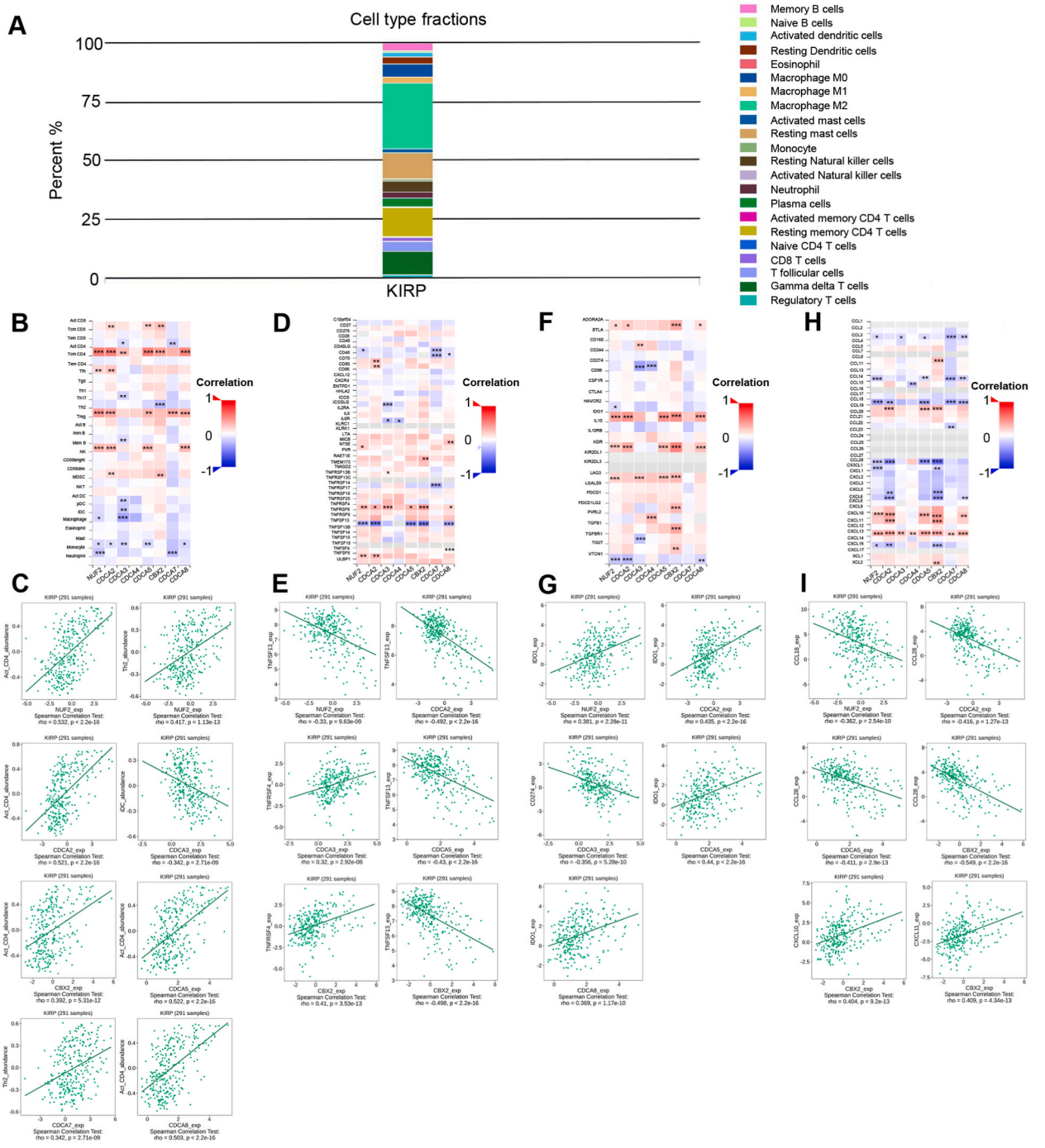

Fig. 5. The correlations between CDCA genes expression and immune molecules. **(A)** The proportions of different immune cell components in KIRP. **(B, C)** The heatmap and scatterplot displayed the correlations between CDCA genes expression and tumor-infiltrating lymphocytes (TILs). **(D, E)** The heatmap and scatterplot displayed the correlations between CDCA genes expression and immunostimulatory molecules. **(F, G)** The heatmap and scatterplot displayed the correlations between CDCA genes expression and immunoinhibitory molecules. **(H, I)** The heatmap and scatterplot displayed the correlations between CDCA genes expression and chemokines. (*$P < 0.05$, **$P < 0.01$, and ***$P < 0.001$ indicated statistical significance).

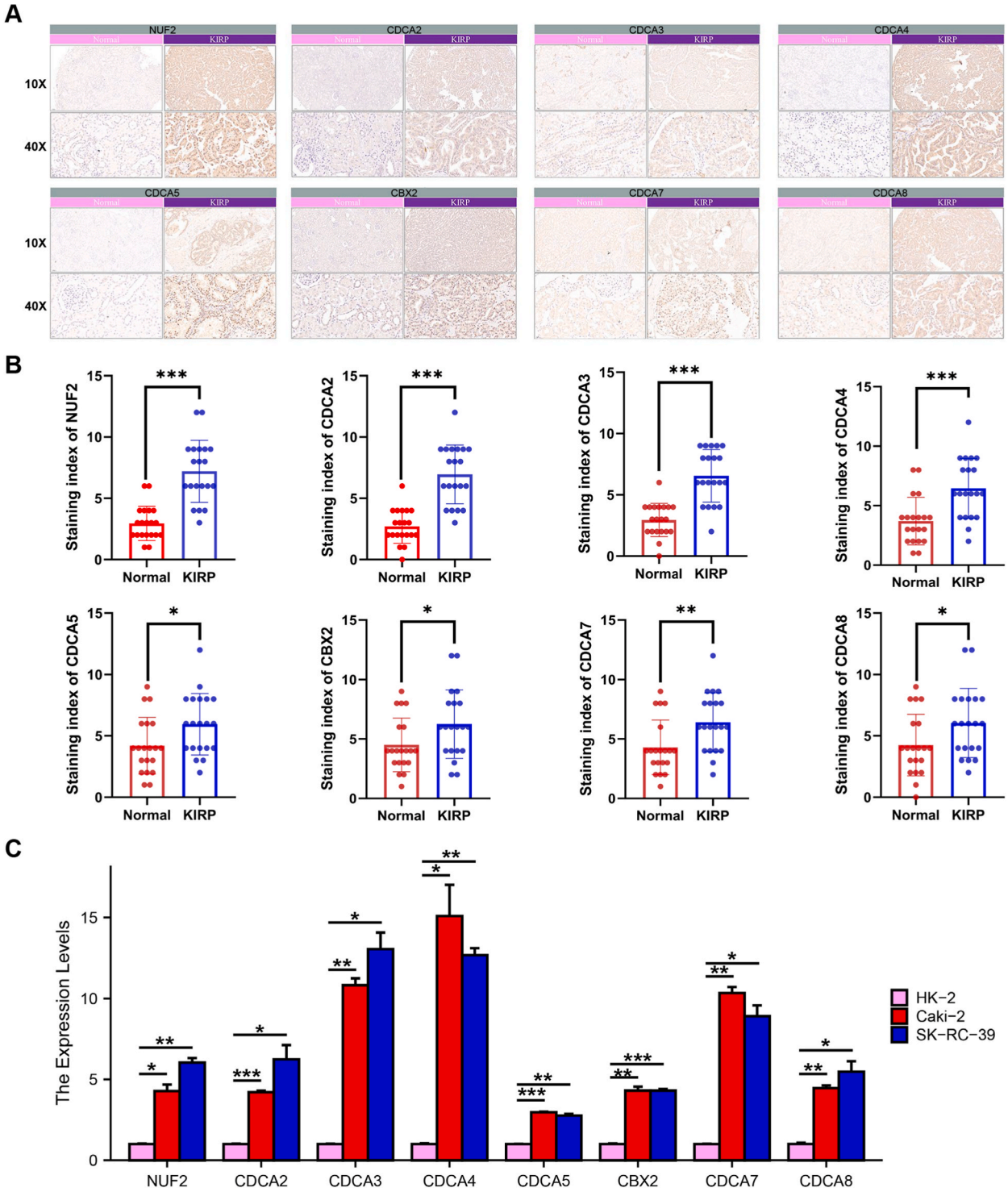

Fig. 6. Validation of CDCAs expression in KIRP tissues by IHC and RT-qPCR. **(A)** IHC images of CDCAs expression in KIRP. **(B)** Staining index of CDCAs in KIRP and normal kidney tissues. **(C)** Bar charts of mRNA level of CDCA genes between HK-2 and Caki-2 and SK-RC-39 cell lines. (*$P <$ 0.05, **$P < 0.01$, and ***$P < 0.001$ indicated statistical significance).

3.4. Construction of a nomogram based on independent risk factors

To identify potential predictors of OS in patients with KIRP, a multivariate Cox regression analysis of relevant clinicopathological characteristics and CDCA genes was conducted using TCGA-KIRP dataset (sTab. 4). As shown in Fig. 3G, pathological T and N staging, NUF2, CDCA2, CDCA3, CDCA5, CBX2, CDCA7, and CDCA8 were associated with poor OS, indicating that these predictors were independent risk factors for KIRP. A nomogram model was established to predict survival outcomes based on the independent risk factors mentioned above (Fig. 3H). The C-index of the nomogram model was 0.810 (0.766–0.855). Calibration curves were utilized to evaluate the nomogram concordance. The calibration plots of the nomogram model demonstrated favorable agreement with the ideal model for the 1-, 3-, and 5-year OS rates (Fig. 3I–K).

3.5. Genomic alterations and co-expression analysis of CDCA genes in KIRP patients

The cBioPortal platform was used to obtain information regarding genomic alterations in the CDCA genes. Among the TCGA-KIRP patients, approximately 7 % (19/280) exhibited alterations in CDCA genes, with amplifications and deep deletions being the most notable. NUF2, CDCA2, CDCA3, CDCA4, CDCA5, CBX2, CDCA7, and CDCA8 were altered in 1.1 %, 0.7 %, 0.4 %, 1.1 %, 0.4 %, 1.1 %, 2.1 %, and 1.8 % of the 280 patients with KIRP , respectively (sFig. 3A). A summary of the genomic alterations in CDCAs in KIRP was shown in sFig. 3B. Similarly, the expression and methylation heatmaps exhibited the degree of mutations and abnormal methylation in CDCA genes (sFig. 3C and D). The mutation rate of CDCA7 in KIRP was the highest among all CDCA genes. CDCA3, CDCA5, and CDCA8 exhibited high DNA methylation (HM450) levels. The chromosomal locations of the CDCA genes were are shown in sFig. 3E. Furthermore, it is possible that the mutation sites present in certain CDCA genes affect their posttranscriptional modifications (PTMs). These mutation sites included K409Q in NUF2, and Y73H and H279Y in CDCA8 (sFig. 3F). Moreover, co-expression analysis showed that CDCA gene family members were closely related (all Cor >0.3, all $P < 0.001$, sFig. 3G).

3.6. PPI network construction, hub genes screening, and functional enrichment analysis

To investigate the potential genes involved in CDCAs-mediated biological pathways in KIRP, a protein interaction network was constructed using the STRING database comprising eight CDCA proteins (Fig. 4A) and 80 frequently interacting neighboring proteins (Fig. 4B). Moreover, our findings, as illustrated in Fig. 4C, revealed that seven hub genes, namely KIFC1, MKI67, KIF4A, KIF11, PRC1, MYBL2, and CEP55, were closely associated with alterations in CDCA genes. Additionally, we identified the three most significant MCODE components from the PPI network between CDCA proteins and their 80 frequently neighboring proteins. We observed that biological functions, such as nuclear chromosome segregation, mitotic sister chromatid segregation, sister chromatid segregation, mitotic cell cycle process and impaired BRCA2 binding to PALB2, were significantly correlated with these MCODE components (Fig. 4D). Subsequently, we performed GO and KEGG functional enrichment analyses of the CDCA genes and their 80 neighboring genes using the DAVID tool. The results are presented in Fig. 4E and F, and sTab. 5. The biological processes involved in nuclear division, organelle fission, mitotic nuclear division, and chromosomal segregation were also significantly enriched (Fig. 4E). Cellular components analysis revealed that CDCA genes were predominantly located in the spindle, chromosome in centromeric region, condensed chromosome, kinetochore, and chromosomal region (Fig. 4E). Molecular function analysis indicated that the CDCA genes were associated with ATPase activity, microtubule motor activity, microtubule binding, motor activity, and tubulin binding (Fig. 4E). Furthermore, KEGG pathway enrichment analysis revealed that alterations in CDCA genes were significantly related to the cell cycle, p53 signaling pathway, cellular senescence, human T-cell leukemia virus 1 infection, oocyte meiosis, homologous recombination, and the Fanconi anemia pathway (Fig. 4F). Notably, the KEGG chord plot demonstrated that CDK1 and CCNB2 were closely related to five crucial KEGG pathways, indicating that CDK1 and CCNB2 may be critical genes in this process (Fig. 4F).

3.7. Correlations between CDCA genes expression and immune molecules

In Fig. 5A, the 100 % stacked bar chart indicates that M2 macrophages, resting memory CD4 T cells, resting mast cells, and gamma delta T cells are the four most predominant infiltrating immune cells in KIRP. Additionally, positive associations were observed between Act_CD4 and the expression of NUF2, CDCA2, CDCA5, CBX2, and CDCA8. Similarly, Th2 cells positively correlated with NUF2 and CDCA7, whereas CDCA3 negatively correlated with iDC (Fig. 5B and C). As illustrated in Fig. 5D and E, among these immunostimulatory molecules, TNFSF13 was negatively correlated with NUF2, CDCA2, CDCA5, and CBX2, whereas TNFRSF4 was positively related to CDCA3 and CBX2. Immunoinhibitory molecules also displayed positive associations, including between IDO1 and NUF2, CDCA2, CDCA5, and CDCA8, whereas CD274 was negatively correlated with CDCA3 (Fig. 5F and G). Furthermore, significant associations were observed between the expression of CDCA genes and chemokines (Fig. 5H and I). Negative correlations were found between CCL18 and NUF2, as well as between CCL28 and CDCA2, CDCA5, and CBX2. In contrast, positive correlations were detected between CBX2, CXCL10, and CXCL11 expressions. Based on the KIRP samples from TCGA database, we further investigated whether CDCAs expression was relevant to MSI, TMB, and immune checkpoints. These results suggest that CDCAs expression was not associated with MSI (all $P > 0.05$, sFig. 4A), and TMB (all $P > 0.05$, sFig. 4B). The immune checkpoint genes CTLA4, HAVCR2, PD-1, PDCD1LG2, and TIGIT were overexpressed in KIRP (all $P < 0.05$, sFig. 4C). Moreover, CDCA2 and CDCA4 were positively related to PD-1 expression (all $P < 0.05$, sFig. 4D); and CBX2 was positively correlated with PD-L1 expression ($P < 0.05$, sFig. 4D). Collectively, these results indicate that CDCA2, CDCA4 and CBX2 are potential immune targets for anti-PD1/PDL1 therapy in KIRP.

3.8. Verification of the CDCAs expression in KIRP tissues by IHC and RT-qPCR

Finally, IHC staining and RT-qPCR were conducted to validate the findings of the bioinformatics analyses. A summary of the features and staining indices of the 20 patients is shown in sTab. 6. As shown in Fig. 6A, the overexpressed CDCAs protein localized mainly in the nucleus. Besides, the staining patterns of CDCAs in tumor and normal tissues were observed, and the results indicated that the protein expression levels of CDCA genes were significantly higher in KIRP tissues than in normal renal tissues (all $P < 0.05$, Fig. 6B). Furthermore, the relative mRNA levels of CDCA genes in the KIRP cell lines Caki-2 and SK-RC-39 were higher than those in the normal kidney cell line HK-2 (all $P < 0.05$, Fig. 6C). These findings are consistent with the results obtained from the bioinformatics analysis of the RNA and protein levels. All in all, these data suggest that CDCA genes may function as oncogenes in KIRP.

4. Discussion

The incidence and mortality rates of kidney cancer increased worldwide [29]. KIRP, the second most prevalent subtype of renal cell carcinoma, is usually detected incidentally during routine physical examinations [30]. Recently, a substantial body of evidence has suggested that CDCA genes are correlated with cancer occurrence, progression, and prognosis [8,16]. However, there are currently few studies on their roles in KIRP. For instance, A study by Li et al. [31] revealed that CDCA3 expression is high and associated with poor prognosis in patients with KIRP. Liu et al. [32] indicated that SNHG6 might facilitate the progression of KIRP by regulating NUF2 and CDCA3. To date, the role of CDCAs in KIRP and whether CDCAs expression is correlated with the immune microenvironment in KIRP remains unclear. Therefore, it is important to investigate the role of CDCAs in KIRP. In this study, we performed comprehensive molecular analyses to explore the expressions, mutations, prognostic value, and biological function of CDCA genes and their correlation with immune infiltration in KIRP using TCGA and GTEx datasets.

To obtain a reliable conclusion, we first explored CDCAs-promoted KIRP progression in TCGA and GTEx databases and then validated this conclusion in our experiments. CDCAs mRNA expressions were higher in KIRP tissues than in normal renal tissues. Similarly, in cell experiments, the contents of CDCA genes were significantly higher in KIRP cell lines than in normal renal cells, which was further verified by IHC. Furthermore, the expression levels of CDCA genes correlated with cancer staging, pathological T, N, and M staging, and gender. The greatest advantage of these common clinicopathological parameters is their easy accessibility, which enables a more comprehensive and informed determination of patient prognosis. Although the prognostic value of CDCA genes has been investigated in ovarian [33], hepatocellular [9], nasopharyngeal [11], and gastric carcinomas [34], this study is the first to systematically explore their prognostic significance in KIRP. Kaplan–Meier analysis indicated that patients with KIRP with elevated CDCA genes expressions had undesirable OS, which was also exhibited in many clinical categories according to subgroup survival analyses. Multivariate Cox regression analysis indicated that NUF2, CDCA2, CDCA3, CDCA5, CBX2, CDCA7, and CDCA8 were independent risk factors for KIRP. A nomogram model with a C-index of 0.810 was developed to predict the survival outcomes of KIRP patients with CDCAs expression. Overall, these findings strongly supported the use of NUF2, CDCA2, CDCA3, CDCA5, CBX2, CDCA7, and CDCA8 as the biomarkers for diagnosis and prognosis of KIRP. Further experimental validation is required to confirm theses results.

Several studies have established that the cell cycle plays a critical role in tumorigenesis and progression, significantly affecting cell proliferation and senescence [35,36]. Moreover, pathologies and cancers have been linked to abnormal nuclear division resulting from chromosome instability caused by the depletion of the biogenesis factor NOP53 [37]. The p53 signaling pathway has been demonstrated to contribute significantly to the regulation of the cell cycle, metabolism, aging and development, reproduction, and suppression of tumor expression, among other functions [38]. In this study, we verified that CDCA genes were associated with process of cell proliferation and involved in cell cycle, p53 signaling pathway and cellular senescence through GO and KEGG functional enrichment analyses. To sum up, our findings are consistent with previous reports indicating that CDCA genes can regulate cell cycle and nuclear division [39].

Previous studies have indicated a correlation between immune infiltration in the tumor microenvironment and the survival rates patients with cancer [40,41]. Specifically, the degree of immune infiltration has been found to be directly related to the prognosis of KIRP [42]. Moreover, previous studies have revealed that the expression of some CDCA gene family members is associated with immune infiltration in certain cancers. For instance, a report from Bai et al. [43] showed that CDCA3 is strongly correlated with poor prognosis and positively associated with the infiltration of $CD8^+$ T cells and Tregs in renal cell carcinoma. In a study by Liu et al. [44], CDCA7 exhibited a significant correlation with immune infiltration, the tumor microenvironment, immune checkpoint molecules, and immune pathways in clear cell renal cell carcinoma (RCC). Similarly, our study found the four most predominant infiltrating immune cells, including M2 macrophages, resting memory CD4 T cells, resting mast cells, and Gamma delta T cells in KIRP. In addition, we found that NUF2 expression was closely associated with lymphocytes of Act_CD4 and Th2, immunostimulatory molecule of TNFSF13, immunoinhibitory molecule of IDO1, and the chemokine CCL18. CDCA2 and CDCA5 expression were discovered to be tightly related to the lymphocytes of Act_CD4, the immunostimulatory molecule TNFSF13, the immunoinhibitory molecule IDO1, and the chemokine CCL28. Moreover, we found a strong correlation between CBX2 expression and the lymphocytes of Act_CD4, immunostimulatory molecules TNFSF13 and TNFRSF4, and chemokines CXCL10 and CXCL11. TNFSF13 (also named as APRIL) is an immunostimulatory molecule, which has been found to be closely correlated with tumorigenesis and as a novel target for cancer immunotherapy [45]. According to previous studies, IDO1, an intracellular heme-containing metalloprotein, plays a crucial role in the production of a range of biologically active secondary metabolites via the KYN pathway [46]. Recently, IDO1 has emerged as a crucial and promising target for cancer immunotherapy, garnering significant attention [47]. These findings confirm our hypothesis and reveal the pivotal role of CDCAs in regulating tumor immunology. Furthermore, our study indicated that CDCA2, CDCA4 and CBX2 could be used as potential immune targets for anti-PD1/PDL1 therapy in KIRP. However, further clinical studies are required to validate the correlation between

CDCAs and immune infiltration in KIRP.

This study had several limitations. First, we evaluated the prognostic value of CDCA genes and established a risk scoring model for patients with KIRP using data primarily sourced from TCGA and GTEx databases. Although the sequencing data from these databases were experimentally validated, further large-scale studies on patients with KIRP from other databases are required to confirm our findings. Second, this study only conducted IHC and RT-PCR experiments, and we did not perform further investigations in cell and animal models. Therefore, more specific downstream pathways of the CDCA genes and their biological mechanisms require further in-depth investigation, and will be explored in our future work.

In conclusion, we conducted a comprehensive assessment of CDCA genes and found that NUF2, CDCA2, CDCA3, CDCA5, CBX2, CDCA7, and CDCA8 may serve as potential biomarkers for KIRP diagnosis and prognosis and that NUF2, CDCA2, CDCA5, and CBX2 are promising targets for KIRP immunotherapy.

Funding

This research did not receive any specific grant from funding agencies in the public, commercial, or not-for-profit sectors.

Data availability statement

All data are included in article/supplementary material/referenced in article.

CRediT authorship contribution statement

Fuping Li: Writing – original draft, Software, Methodology, Investigation, Formal analysis, Conceptualization. **Zhenheng Wu:** Writing – original draft, Validation, Data curation. **Zhiyong Du:** Software, Data curation. **Qiming Ke:** Visualization, Validation. **Yuxiang Fu:** Visualization, Software. **Jiali Zhan:** Writing – review & editing, Supervision, Conceptualization.

Declaration of competing interest

All authors (Fuping Li, Zhenheng Wu, Zhiyong Du, Qiming Ke, Yuxiang Fu and Jiali Zhan) have read and approved the content, and agree to submit it for consideration for publication in your journal. There are no ethical/legal conflicts involved in the article.

Appendix A. Supplementary data

Supplementary data to this article can be found online at https://doi.org/10.1016/j.heliyon.2024.e33045.

References

[1] M. de Vries-Brilland, D.F. McDermott, C. Suárez, T. Powles, M. Gross-Goupil, A. Ravaud, R. Flippot, B. Escudier, L. Albigès, Checkpoint inhibitors in metastatic papillary renal cell carcinoma. https://doi.org/10.1016/j.ctrv.2021.102228.

[2] A.J. Armstrong, S. Halabi, T. Eisen, S. Broderick, W.M. Stadler, R.J. Jones, J.A. Garcia, U.N. Vaishampayan, J. Picus, R.E. Hawkins, J.D. Hainsworth, C. K. Kollmannsberger, T.F. Logan, I. Puzanov, L.M. Pickering, C.W. Ryan, A. Protheroe, C.M. Lusk, S. Oberg, D.J. George, Everolimus versus sunitinib for patients with metastatic non-clear cell renal cell carcinoma (ASPEN): a multicentre, open-label, randomised phase 2 trial, Lancet Oncol. 17 (2016) 378–388, https://doi.org/10.1016/S1470-2045(15)00515-X.

[3] H. Tachibana, T. Kondo, H. Ishihara, H. Fukuda, K. Yoshida, T. Takagi, J. Izuka, H. Kobayashi, K. Tanabe, Modest efficacy of nivolumab plus ipilimumab in patients with papillary renal cell carcinoma, Jpn. J. Clin. Oncol. 51 (2021) 646–653, https://doi.org/10.1093/jjco/hyaa229.

[4] M.L. Eich, A. Chaux, M.A. Mendoza Rodriguez, G. Guner, D. Taheri, M.D.C. Rodriguez Pena, R. Sharma, M.E. Allaf, G.J. Netto, Tumour immune microenvironment in primary and metastatic papillary renal cell carcinoma, Histopathology 76 (2020) 423–432, https://doi.org/10.1111/his.13987.

[5] S.J. Habib, S.P. Acebron, Wnt signalling in cell division: from mechanisms to tissue engineering, Trends Cell Biol. 32 (2022) 1035–1048, https://doi.org/10.1016/j.tcb.2022.05.006.

[6] S. Preston-Martin, M.C. Pike, R.K. Ross, P.A. Jones, B.E. Henderson, Increased cell division as a cause of human cancer, Cancer Res. 50 (1990) 7415–7421.

[7] G. Vader, S.M. Lens, The Aurora kinase family in cell division and cancer, Biochim. Biophys. Acta 1786 (2008) 60–72, https://doi.org/10.1016/j.bbcan.2008.07.003.

[8] R. Leng, Y. Meng, X. Sun, Y. Zhao, NUF2 overexpression contributes to epithelial ovarian cancer progression via ERBB3-mediated PI3K-AKT and MAPK signaling axes, Front. Oncol. 12 (2022) 1057198, https://doi.org/10.3389/fonc.2022.1057198.

[9] Z.H. Wu, D.L. Yang, L. Wang, J. Liu, Epigenetic and immune-cell infiltration changes in the tumor microenvironment in hepatocellular carcinoma, Front. Immunol. 12 (2021) 793343, https://doi.org/10.3389/fimmu.2021.793343.

[10] P.L. Clermont, F. Crea, Y.T. Chiang, D. Lin, A. Zhang, J.Z. Wang, A. Parolia, R. Wu, H. Xue, Y. Wang, J. Ding, K.L. Thu, W.L. Lam, S.P. Shah, C.C. Collins, Y. Wang, C.D. Helgason, Identification of the epigenetic reader CBX2 as a potential drug target in advanced prostate cancer, Clin Epigenetics 8 (2016) 16, https://doi.org/10.1186/s13148-016-0182-9.

[11] D. Jiang, Y. Li, J. Cao, L. Sheng, X. Zhu, M. Xu, Cell division cycle-associated genes are potential immune regulators in nasopharyngeal carcinoma, Front. Oncol. 12 (2022) 779175, https://doi.org/10.3389/fonc.2022.779175.

[12] D.G. Pique, C. Montagna, J.M. Greally, J.C. Mar, A novel approach to modelling transcriptional heterogeneity identifies the oncogene candidate CBX2 in invasive breast carcinoma, Br. J. Cancer 120 (2019) 746–753, https://doi.org/10.1038/s41416-019-0387-8.

[13] C.H. Wong, U.K. Lou, Y. Li, S.L. Chan, J.H. Tong, K.F. To, Y. Chen, CircFOXK2 promotes growth and Metastasis of pancreatic ductal adenocarcinoma by complexing with RNA-binding proteins and sponging MiR-942, Cancer Res. 80 (2020) 2138–2149, https://doi.org/10.1158/0008-5472.CAN-19-3268.

[14] Y. Guo, K. Zhou, X. Zhuang, J. Li, X. Shen, CDCA7-regulated inflammatory mechanism through TLR4/NF-kappaB signaling pathway in stomach adenocarcinoma, Biofactors 47 (2021) 865–878, https://doi.org/10.1002/biof.1773.
[15] J. Wu, M. Cui, J. Wang, J. Fan, S. Liu, W. Lou, CDCA3 promotes the proliferation and migration of hypopharyngeal squamous cell carcinoma cells by activating the Akt/mTOR pathway, Biotechnol. Genet. Eng. Rev. (2023) 1–19, https://doi.org/10.1080/02648725.2023.2187876.
[16] M.N. Adams, J.T. Burgess, Y. He, K. Gately, C. Snell, S.D. Zhang, J.D. Hooper, D.J. Richard, K.J. O'Byrne, Expression of CDCA3 is a prognostic biomarker and potential therapeutic target in non-small cell lung cancer, J. Thorac. Oncol. 12 (2017) 1071–1084, https://doi.org/10.1016/j.jtho.2017.04.018.
[17] Q. Tang, D. Pan, C. Xu, L. Chen, Identification of molecular subtypes based on chromatin regulator and tumor microenvironment infiltration characterization in papillary renal cell carcinoma, J. Cancer Res. Clin. Oncol. 149 (2023) 231–245, https://doi.org/10.1007/s00432-022-04482-4.
[18] H. Lee, J. Palm, S.M. Grimes, H.P. Ji, The Cancer Genome Atlas Clinical Explorer: a web and mobile interface for identifying clinical-genomic driver associations, Genome Med. 7 (2015) 112, https://doi.org/10.1186/s13073-015-0226-3.
[19] G.T. Consortium, The genotype-tissue expression (GTEx) project, Nat. Genet. 45 (2013) 580–585, https://doi.org/10.1038/ng.2653.
[20] H. Parkinson, M. Kapushesky, M. Shojatalab, N. Abeygunawardena, R. Coulson, A. Farne, E. Holloway, N. Kolesnykov, P. Lilja, M. Lukk, R. Mani, T. Rayner, A. Sharma, E. William, U. Sarkans, A. Brazma, ArrayExpress–a public database of microarray experiments and gene expression profiles, Nucleic Acids Res. 35 (2007) D747–D750, https://doi.org/10.1093/nar/gkl995.
[21] E. Cerami, J. Gao, U. Dogrusoz, B.E. Gross, S.O. Sumer, B.A. Aksoy, A. Jacobsen, C.J. Byrne, M.L. Heuer, E. Larsson, Y. Antipin, B. Reva, A.P. Goldberg, C. Sander, N. Schultz, The cBio cancer genomics portal: an open platform for exploring multidimensional cancer genomics data, Cancer Discov. 2 (2012) 401–404, https://doi.org/10.1158/2159-8290.CD-12-0095.
[22] B. Ru, C.N. Wong, Y. Tong, J.Y. Zhong, S.S.W. Zhong, W.C. Wu, K.C. Chu, C.Y. Wong, C.Y. Lau, I. Chen, N.W. Chan, J. Zhang, TISIDB: an integrated repository portal for tumor-immune system interactions, Bioinformatics 35 (2019) 4200–4202, https://doi.org/10.1093/bioinformatics/btz210.
[23] Z. Tang, B. Kang, C. Li, T. Chen, Z. Zhang, GEPIA2: an enhanced web server for large-scale expression profiling and interactive analysis, Nucleic Acids Res. 47 (2019) W556–W560, https://doi.org/10.1093/nar/gkz430.
[24] J. Liu, T. Lichtenberg, K.A. Hoadley, L.M. Poisson, A.J. Lazar, A.D. Cherniack, A.J. Kovatich, C.C. Benz, D.A. Levine, A.V. Lee, L. Omberg, D.M. Wolf, C. D. Shriver, V. Thorsson, N. Cancer Genome Atlas Research, H. Hu, An integrated TCGA pan-cancer clinical data resource to drive high-quality survival outcome analytics, Cell 173 (2018) 400–416 e411, https://doi.org/10.1016/j.cell.2018.02.052.
[25] D. Szklarczyk, A.L. Gable, D. Lyon, A. Junge, S. Wyder, J. Huerta-Cepas, M. Simonovic, N.T. Doncheva, J.H. Morris, P. Bork, L.J. Jensen, C.V. Mering, STRING v11: protein-protein association networks with increased coverage, supporting functional discovery in genome-wide experimental datasets, Nucleic Acids Res. 47 (2019) D607–D613, https://doi.org/10.1093/nar/gky1131.
[26] Y. Zhou, B. Zhou, L. Pache, M. Chang, A.H. Khodabakhshi, O. Tanaseichuk, C. Benner, S.K. Chanda, Metascape provides a biologist-oriented resource for the analysis of systems-level datasets, Nat. Commun. 10 (2019) 1523, https://doi.org/10.1038/s41467-019-09234-6.
[27] D.W. Huang, B.T. Sherman, Q. Tan, J.R. Collins, W.G. Alvord, J. Roayaei, R. Stephens, M.W. Baseler, H.C. Lane, R.A. Lempicki, The DAVID Gene Functional Classification Tool: a novel biological module-centric algorithm to functionally analyze large gene lists, Genome Biol. 8 (2007) R183, https://doi.org/10.1186/gb-2007-8-9-r183.
[28] P. Charoentong, F. Finotello, M. Angelova, C. Mayer, M. Efremova, D. Rieder, H. Hackl, Z. Trajanoski, Pan-cancer immunogenomic analyses reveal genotype-immunophenotype relationships and predictors of response to checkpoint blockade, Cell Rep. 18 (2017) 248–262, https://doi.org/10.1016/j.celrep.2016.12.019.
[29] Z.Y. Zhang, S.L. Zhang, H.L. Chen, Y.Q. Mao, Z.M. Li, C.Y. Kong, B. Han, J. Zhang, Y.H. Chen, W. Xue, W. Zhai, L.S. Wang, The up-regulation of NDRG1 by HIF counteracts the cancer-promoting effect of HIF in VHL-deficient clear cell renal cell carcinoma, Cell Prolif. 53 (2020) e12853, https://doi.org/10.1111/cpr.12853.
[30] M.B. Amin, M.B. Amin, P. Tamboli, J. Javidan, H. Stricker, M. de-Peralta Venturina, A. Deshpande, M. Menon, Prognostic impact of histologic subtyping of adult renal epithelial neoplasms: an experience of 405 cases, Am. J. Surg. Pathol. 26 (2002) 281–291, https://doi.org/10.1097/00000478-200203000-00001.
[31] H. Li, M. Li, C. Yang, F. Guo, S. Deng, L. Li, T. Ma, J. Yan, H. Wu, X. Li, Prognostic value of CDCA3 in kidney renal papillary cell carcinoma, Aging (Albany NY) 13 (2021) 25466–25483, https://doi.org/10.18632/aging.203767.
[32] Y. Liu, X. Cheng, P. Xi, Z. Zhang, T. Sun, B. Gong, Bioinformatic analysis highlights SNHG6 as a putative prognostic biomarker for kidney renal papillary cell carcinoma, BMC Urol. 23 (2023) 54, https://doi.org/10.1186/s12894-023-01218-5.
[33] C. Chen, S. Chen, M. Luo, H. Yan, L. Pang, C. Zhu, W. Tan, Q. Zhao, J. Lai, H. Li, The role of the CDCA gene family in ovarian cancer, Ann. Transl. Med. 8 (2020) 190, https://doi.org/10.21037/atm.2020.01.99.
[34] P. Lu, W. Cheng, K. Fang, B. Yu, Multidimensional study of cell division cycle-associated proteins with prognostic value in gastric carcinoma, Bosn. J. Basic Med. Sci. 22 (2022) 64–76, https://doi.org/10.17305/bjbms.2021.5783.
[35] M.B. Kastan, J. Bartek, Cell-cycle checkpoints and cancer, Nature 432 (2004) 316–323, https://doi.org/10.1038/nature03097.
[36] K. Zheng, Z. He, K. Kitazato, Y. Wang, Selective autophagy regulates cell cycle in cancer therapy, Theranostics 9 (2019) 104–125, https://doi.org/10.7150/thno.30308.
[37] S. Lee, Y.M. Ahn, J.Y. Kim, Y.E. Cho, J.H. Park, Downregulation of NOP53 ribosome biogenesis factor leads to abnormal nuclear division and chromosomal instability in human cervical cancer cells, Pathol. Oncol. Res. 26 (2020) 453–459, https://doi.org/10.1007/s12253-018-0531-4.
[38] H. Khan, M. Reale, H. Ullah, A. Sureda, S. Tejada, Y. Wang, Z.J. Zhang, J. Xiao, Anti-cancer effects of polyphenols via targeting p53 signaling pathway: updates and future directions, Biotechnol. Adv. 38 (2020) 107385, https://doi.org/10.1016/j.biotechadv.2019.04.007.
[39] H. Izumi, T. Wakasugi, S. Shimajiri, A. Tanimoto, Y. Sasaguri, E. Kashiwagi, Y. Yasuniwa, M. Akiyama, B. Han, Y. Wu, T. Uchiumi, T. Arao, K. Nishio, R. Yamazaki, K. Kohno, Role of ZNF143 in tumor growth through transcriptional regulation of DNA replication and cell-cycle-associated genes, Cancer Sci. 101 (2010) 2538–2545, https://doi.org/10.1111/j.1349-7006.2010.01725.x.
[40] W.H. Fridman, F. Pages, C. Sautes-Fridman, J. Galon, The immune contexture in human tumours: impact on clinical outcome, Nat. Rev. Cancer 12 (2012) 298–306, https://doi.org/10.1038/nrc3245.
[41] S. Zheng, J.Y. Liang, Y. Tang, J. Xie, Y. Zou, A. Yang, N. Shao, X. Kuang, F. Ji, X. Liu, W. Tian, W. Xiao, Y. Lin, Dissecting the role of cancer-associated fibroblast-derived biglycan as a potential therapeutic target in immunotherapy resistance: a tumor bulk and single-cell transcriptomic study, Clin. Transl. Med. 13 (2023) e1189, https://doi.org/10.1002/ctm2.1189.
[42] S. Zhang, E. Zhang, J. Long, Z. Hu, J. Peng, L. Liu, F. Tang, L. Li, Y. Ouyang, Z. Zeng, Immune infiltration in renal cell carcinoma, Cancer Sci. 110 (2019) 1564–1572, https://doi.org/10.1111/cas.13996.
[43] Y. Bai, S. Liao, Z. Yin, B. You, D. Lu, Y. Chen, D. Chen, Y. Wu, CDCA3 predicts poor prognosis and affects CD8(+) T cell infiltration in renal cell carcinoma, J Oncol 2022 (2022) 6343760, https://doi.org/10.1155/2022/6343760.
[44] S. Liu, Y. Wang, C. Miao, Q. Xing, Z. Wang, High expression of CDCA7 predicts poor prognosis for clear cell renal cell carcinoma and explores its associations with immunity, Cancer Cell Int. 21 (2021) 140, https://doi.org/10.1186/s12935-021-01834-x.
[45] K.H. Nowacka, E. Jablonska, Role of the APRIL molecule in solid tumors, Cytokine Growth Factor Rev. 61 (2021) 38–44, https://doi.org/10.1016/j.cytogfr.2021.08.001.
[46] M. Platten, E.A.A. Nollen, U.F. Rohrig, F. Fallarino, C.A. Opitz, Tryptophan metabolism as a common therapeutic target in cancer, neurodegeneration and beyond, Nat. Rev. Drug Discov. 18 (2019) 379–401, https://doi.org/10.1038/s41573-019-0016-5.
[47] L. Zhai, E. Ladomersky, A. Lenzen, B. Nguyen, R. Patel, K.L. Lauing, M. Wu, D.A. Wainwright, Ido1 in cancer: a Gemini of immune checkpoints, Cell. Mol. Immunol. 15 (2018) 447–457, https://doi.org/10.1038/cmi.2017.143.